Journal of Zhejiang University SCIENCE
ISSN 1009-3095
http://www.zju.edu.cn/jzus
E-mail: jzus@zju.edu.cn

Analytical modelling and free vibration analysis of piezoelectric bimorphs*

ZHOU Yan-guo (周燕国)†, CHEN Yun-min (陈云敏)†‡, DING Hao-jiang (丁皓江)

(*Department of Civil Engineering, Zhejiang University, Hangzhou 310027, China*)

†E-mail: qzking@zju.edu.cn; cym@civil.zju.edu.cn

Received Mar. 1, 2005; revision accepted Apr. 20, 2005

Abstract: An efficient and accurate analytical model for piezoelectric bimorph based on the improved first-order shear deformation theory (FSDT) is developed in this work. The model combines the equivalent single-layer approach for mechanical displacements and a layerwise-type modelling of the electric potential. Particular attention is devoted to the boundary conditions on the outside faces and to the interface continuity conditions of the bimorphs for the electromechanical variables. Shear correction factor (k) is introduced to modify both the shear stress and the electric displacement of each layer. And the detailed mathematical derivations are presented. Free vibration problem of simply supported piezoelectric bimorphs with series or parallel arrangement is investigated for the closed circuit condition, and the results for different length-to-thickness ratios are compared with those obtained from the exact 2D solution. Excellent agreements between the present model prediction with k=8/9 and the exact solutions are observed for the resonant frequencies.

Key words: Piezoelectric bimorph, Analytical model, Free vibration, Shear correction factor, First-order shear deformation theory

doi:10.1631/jzus.2005.A0938 **Document code:** A **CLC number:** O326; O343.8; TU411.8

INTRODUCTION

Piezoelectric bimorphs (or benders), a special type of piezoelectric device, which can produce flexural deformation significantly larger than the length or thickness deformation of the individual piezoelectric layers, have been widely used as electroacoustic transducers, medical devices and micro-robot due to their characteristics of easy miniaturization, high positioning accuracy, sensitive response, and large displacement (e.g., Shirley and Hampton, 1978; Ha and Kim, 2002; Zhou *et al*., 2005). Typically, two possible arrangements of the piezoelectric elements are adopted. The first, called parallel (or Y-P), means that two piezoelectric elements are epoxied to a center conductor in an orientation that have the same poling direction, and the outer faces are coated with two conductive electrodes. The second is known as series (or X-P) in which two piezoelectric elements with opposite poling directions are directly bonded, and then covered by two surface electrodes. The application of an electric field across the two layers of the bimorph causes one layer to expand, while the other layer contracts. This is the working principle of bimorphs. To design and use such bimorphs rationally, it is crucial to understand their coupled electromechanical behaviors through effective modelling.

In the past decades, the research of piezoelectric bimorphs has experienced tremendous growth (Rao and Sunar, 1994; Chee *et al*., 1998; He *et al*., 2000; Lim *et al*., 2001; Wang, 2004). However, most of the existing models are either inaccurate or overcomplicated (Gopinathan *et al*., 2000). The present work attempts to develop a consistent, yet comprehensive approach to piezoelectric bimorphs. The model combines an equivalent single-layer theory for the me-

‡Corresponding author
*Project (Nos. 10472102 and 10372089) supported by the National Natural Science Foundation of China

chanical displacements with layerwise-type approximation for the electric potential (Fernandes and Pouget, 2003). First-order shear deformation theory (FSDT) kinematics and quadratic electric potentials are assumed in developing the analytical solution. Mechanical displacement and electric potential Fourier-series amplitudes are treated as fundamental variables, and full electromechanical coupling is maintained. Numerical analysis of the simply supported bimorphs under free vibration conditions are presented for different length-to-thickness ratios (i.e., aspect ratio), and the results are verified by those obtained from the exact 2D solution.

BEAM MODEL AND FIELD APPROXIMATION

The piezoelectric bimorph structure studied can be treated as a symmetric lamina in the state of plane stress (Fig.1). The bimorph of unit width is comprised of two identical piezoelectric layers with length l and thickness h for each piezoelectric layer. All layers are considered mechanically and electrically perfectly bonded.

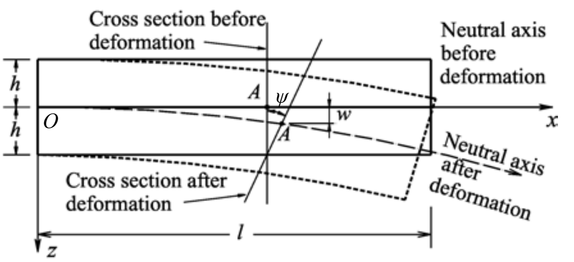

Fig.1 Piezoelectric bimorph: coordinates and geometry

Basic equations of piezoelectricity

The linear field equations of motion for orthotropic piezoelectric media under 2D plane stress assumptions are given by (Sosa and Castro, 1993; Ding *et al*., 1997):

$$\frac{\partial \sigma_x}{\partial x}+\frac{\partial \tau_{xz}}{\partial z}+f_x=\rho\frac{\partial^2 u_x}{\partial t^2},\ \frac{\partial D_x}{\partial x}+\frac{\partial D_z}{\partial z}=0,$$
$$\frac{\partial \tau_{xz}}{\partial x}+\frac{\partial \sigma_z}{\partial z}+f_z=\rho\frac{\partial^2 u_z}{\partial t^2} \tag{1}$$

where ρ is the mass density of piezoelectric material; u_x and u_z are the displacement components of the bimorph in the longitudinal and transverse directions, respectively; f_x and f_z are the body forces; σ_x, σ_z, τ_{xz}, D_x and D_z represent the stress components, electric displacement components, which satisfy the linear constitutive equations of piezoelectricity as

$$\sigma_x=\bar{c}_{11}\varepsilon_x+\bar{c}_{13}\varepsilon_z-(-1)^r\bar{e}_{31}E_z \tag{2a}$$
$$\sigma_z=\bar{c}_{13}\varepsilon_x+\bar{c}_{33}\varepsilon_z-(-1)^r\bar{e}_{33}E_z \tag{2b}$$
$$\tau_{xz}=c_{55}\gamma_{xz}-(-1)^r e_{15}E_x \tag{2c}$$
$$D_z=(-1)^r\left(\bar{e}_{31}\varepsilon_x+\bar{e}_{33}\varepsilon_z\right)+\bar{\varepsilon}_{33}E_z \tag{2d}$$
$$D_x=(-1)^r e_{15}\gamma_{xz}+\varepsilon_{11}E_x \tag{2e}$$

where r is an integer and r=2 if the layer poling direction coincides with the coordinate axes and otherwise r=1; ε_x, ε_z, γ_{xz}, E_x and E_z are strain and electric field intensity components, which relate to the displacement components and electric potential by

$$\varepsilon_x=\frac{\partial u_x}{\partial x},\ \varepsilon_z=\frac{\partial u_z}{\partial z},\ \gamma_{xz}=\frac{\partial u_x}{\partial z}+\frac{\partial u_z}{\partial x} \tag{3a}$$
$$E_x=-\frac{\partial \phi}{\partial x},\ E_z=-\frac{\partial \phi}{\partial z} \tag{3b}$$

It should be noted here that $\bar{c}_{11}$, $\bar{c}_{13}$, $\bar{c}_{33}$, $\bar{e}_{31}$, $\bar{e}_{33}$ and $\bar{\varepsilon}_{33}$ in Eq.(2) are the reduced material constants of the piezoelectric medium under 2D plane stress assumptions (See Appendix A).

FSDT kinematics field approximation

According to first-order shear deformation theory (Timoshenko *et al*., 1974), the effect of shear deformation (and rotary inertia in dynamic analysis) cannot be omitted, so the mechanical displacements are assumed as follows:

$$u_z(x,z,t)=w(x,t),\ u_x(x,z,t)=-z\psi(x,t) \tag{4}$$

where w is the displacement of the bimorph's neutral axis; and ψ is the bending rotations of the vertical lines perpendicular to the neutral axis (Fig.1).

Substituting Eq.(4) into Eq.(3a), we get the strain of the piezoelectric layer as

$$\varepsilon_x=-z\frac{\partial \psi}{\partial x},\ \gamma_{xz}=-\psi+\frac{\partial w}{\partial x} \tag{5}$$

In general, the electric potential is associated with the applied electric potential $G(x, z, t)$ and the induced electric potential by elastic deformation $\varphi(x, z, t)$ (Fig.2). Now, we propose the following functions

$$\begin{aligned}\phi(x,z,t) &= G(x,z,t) + \varphi(x,z,t) \\ &= g(z)V(x,t) + f(z)\Phi(x,t)\end{aligned} \tag{6}$$

where $V(x, t)$ is the amplitude of $G(x, z, t)$ at surfaces, and $g(z)$ is the linear distribution function along the thickness direction of this applied electric potential; $f(z)$ is the through-the-thickness distribution function of $\varphi(x, z, t)$, and $\Phi(x, t)$ is the electric potential amplitude on the midline of the piezoelectric layer.

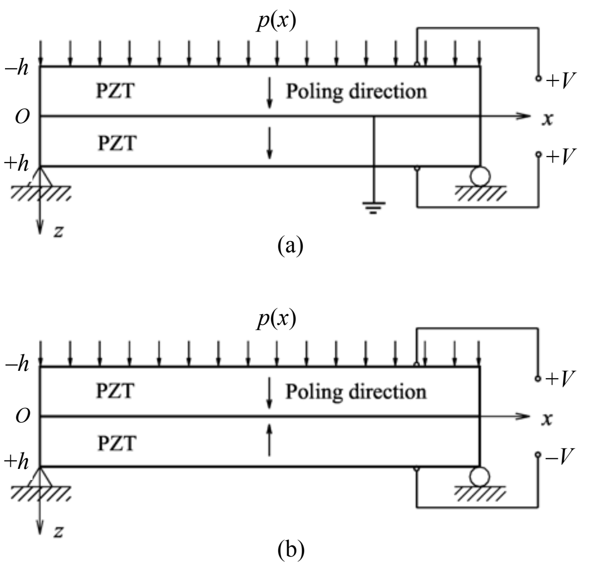

Fig.2 Piezoelectric bimorph settings: (a) parallel arrangement (Y-P); (b) series arrangement (X-P)

According to the studies of Smits *et al.*(1991), Yang (1999), and Wang *et al.*(2001), the electric potential functions mentioned above can be approximated, in view of the settings in Fig.2, as

$$g(z) = \begin{cases} (-1)^r(-z/h), & -h \le z \le 0 \\ (-1)^r(z/h), & 0 < z \le +h \end{cases} \tag{7a}$$

$$f(z) = \begin{cases} (-1)^r\left[1 - \left(\dfrac{z+h/2}{h/2}\right)^2\right], & -h \le z \le 0 \\ (-1)^r\left[1 - \left(\dfrac{z-h/2}{h/2}\right)^2\right], & 0 < z \le +h \end{cases} \tag{7b}$$

where

$$r = \begin{cases} 2, & -h \le z \le 0 \\ 2, & 0 < z \le +h \end{cases} \quad \text{(Y-P)}$$
$$r = \begin{cases} 2, & -h \le z \le 0 \\ 1, & 0 < z \le +h \end{cases} \quad \text{(X-P)} \tag{8}$$

Substituting Eqs.(6) and (7) into Eq.(3b) yields the following electric field intensity components

$$E_x = \begin{cases} (-1)^r\left\{-\left[1-\left(\dfrac{z+h/2}{h/2}\right)^2\right]\dfrac{\partial\Phi}{\partial x} + \dfrac{z}{h}\dfrac{\partial V}{\partial x}\right\}, \\ \qquad -h \le z \le 0 \\ (-1)^r\left\{-\left[1-\left(\dfrac{z-h/2}{h/2}\right)^2\right]\dfrac{\partial\Phi}{\partial x} - \dfrac{z}{h}\dfrac{\partial V}{\partial x}\right\}, \\ \qquad 0 < z \le +h \end{cases} \tag{9a}$$

$$E_z = \begin{cases} (-1)^r\left(8\dfrac{z+h/2}{h^2}\Phi + \dfrac{1}{h}V\right), & -h \le z \le 0 \\ (-1)^r\left(8\dfrac{z-h/2}{h^2}\Phi - \dfrac{1}{h}V\right), & 0 < z \le +h \end{cases} \tag{9b}$$

And the zero normal stress assumption in FSDT leads to the solution of σ_z=0 in Eq.(2b) for ε_z, as

$$\varepsilon_z = -\frac{\bar{c}_{13}}{\bar{c}_{33}}\varepsilon_x + (-1)^r\frac{\bar{e}_{33}}{\bar{c}_{33}}E_z \tag{10}$$

Then substituting the results and Eq.(5) into Eq.(2), and incorporating Eqs.(9) and (10), yields the electromechanical variables for either type of arrangement under FSDT assumptions

$$\sigma_x = \begin{cases} -\left(\bar{e}_{31} - \dfrac{\bar{c}_{13}}{\bar{c}_{33}}\bar{e}_{33}\right)\left[8\dfrac{z+h/2}{h^2}\Phi + \dfrac{1}{h}V\right] - \left(\bar{c}_{11} - \dfrac{\bar{c}_{13}^2}{\bar{c}_{33}}\right)z\dfrac{\partial\psi}{\partial x}, \\ \qquad -h \le z \le 0 \\ -\left(\bar{e}_{31} - \dfrac{\bar{c}_{13}}{\bar{c}_{33}}\bar{e}_{33}\right)\left[8\dfrac{z-h/2}{h^2}\Phi - \dfrac{1}{h}V\right] - \left(\bar{c}_{11} - \dfrac{\bar{c}_{13}^2}{\bar{c}_{33}}\right)z\dfrac{\partial\psi}{\partial x}, \\ \qquad 0 < z \le +h \end{cases} \tag{11a}$$

$$\tau_{xz}=\begin{cases}-e_{15}\left\{-\left[1-\left(\dfrac{z+h/2}{h/2}\right)^2\right]\dfrac{\partial\Phi}{\partial x}+\dfrac{z}{h}\dfrac{\partial V}{\partial x}\right\}+c_{55}\left(-\psi+\dfrac{\partial w}{\partial x}\right), & -h\le z\le 0\\ -e_{15}\left\{-\left[1-\left(\dfrac{z-h/2}{h/2}\right)^2\right]\dfrac{\partial\Phi}{\partial x}-\dfrac{z}{h}\dfrac{\partial V}{\partial x}\right\}+c_{55}\left(-\psi+\dfrac{\partial w}{\partial x}\right), & 0<z\le +h\end{cases} \quad (11b)$$

$$D_x=\begin{cases}(-1)^r\varepsilon_{11}\left\{-\left[1-\left(\dfrac{z+h/2}{h/2}\right)^2\right]\dfrac{\partial\Phi}{\partial x}+\dfrac{z}{h}\dfrac{\partial V}{\partial x}\right\}+(-1)^r e_{15}\left(-\psi+\dfrac{\partial w}{\partial x}\right), & -h\le z\le 0\\ (-1)^r\varepsilon_{11}\left\{-\left[1-\left(\dfrac{z-h/2}{h/2}\right)^2\right]\dfrac{\partial\Phi}{\partial x}-\dfrac{z}{h}\dfrac{\partial V}{\partial x}\right\}+(-1)^r e_{15}\left(-\psi+\dfrac{\partial w}{\partial x}\right), & 0<z\le +h\end{cases} \quad (11c)$$

$$D_z=\begin{cases}(-1)^r\left(\dfrac{\bar{e}_{33}^2}{\bar{c}_{33}}+\bar{\varepsilon}_{33}\right)\left[8\dfrac{z+h/2}{h^2}\Phi+\dfrac{1}{h}V\right]-(-1)^r\left(\bar{e}_{31}-\dfrac{\bar{c}_{13}}{\bar{c}_{33}}\bar{e}_{33}\right)z\dfrac{\partial\psi}{\partial x}, & -h\le z\le 0\\ (-1)^r\left(\dfrac{\bar{e}_{33}^2}{\bar{c}_{33}}+\bar{\varepsilon}_{33}\right)\left[8\dfrac{z-h/2}{h^2}\Phi-\dfrac{1}{h}V\right]-(-1)^r\left(\bar{e}_{31}-\dfrac{\bar{c}_{13}}{\bar{c}_{33}}\bar{e}_{33}\right)z\dfrac{\partial\psi}{\partial x}, & 0<z\le +h\end{cases} \quad (11d)$$

Eq.(11) indicates that there is no fundamental difference between the parallel and series bimorphs under FSDT assumptions since the electromechanical variables are almost the same except for the electric components symmetry.

EQUATIONS OF MOTION FOR BIMORPHS

Based on Timoshenko's beam theory and the charge conservation law, the motion equations of piezoelectric bimorph (e.g., the parallel arrangement) in Eq.(1) can be satisfied approximately by applying integration over the cross section as

$$\frac{\partial M_x}{\partial x}-Q_x-\int_{-h}^{h}\rho z\frac{\partial^2 u_x}{\partial t^2}\mathrm{d}z=m \quad (12)$$

$$-\frac{\partial Q_x}{\partial x}+\int_{-h}^{h}\rho\frac{\partial^2 u_z}{\partial t^2}\mathrm{d}z=p \quad (13)$$

$$\int_0^h\left(\frac{\partial D_x}{\partial x}+\frac{\partial D_z}{\partial z}\right)\mathrm{d}z=0 \text{ or } \int_{-h}^0\left(\frac{\partial D_x}{\partial x}+\frac{\partial D_z}{\partial z}\right)\mathrm{d}z=0 \quad (14)$$

where m and p are the corresponding externally applied couple and force; M_x and Q_x are the bending moment and shear force, which can be expressed as

$$M_x=\int_{-h}^0 z\sigma_x\mathrm{d}z+\int_0^h z\sigma_x\mathrm{d}z \quad (15a)$$

$$Q_x=\int_{-h}^0 \tau_{xz}\mathrm{d}z+\int_0^h \tau_{xz}\mathrm{d}z \quad (15b)$$

Substituting the stress components in Eq.(11) into Eq.(15), yields the expressions for the shear force and moment. Then substituting these resultants into Eqs.(12) and (13), and substituting the electric displacements in Eq.(11) into Eq.(14), with shear coefficient k defined in FSDT, yields the motion equations

$$-b_{11}\frac{\partial w}{\partial x}+\left(b_{21}\frac{\partial^2}{\partial x^2}-b_{12}-b_{41}\frac{\partial^2}{\partial t^2}\right)\psi+(b_{22}-b_{13})\frac{\partial\Phi}{\partial x}=m+(b_{14}-b_{23})\frac{\partial V}{\partial x} \quad (16)$$

$$-\left(b_{11}\frac{\partial^2}{\partial x^2}-b_{42}\frac{\partial^2}{\partial t^2}\right)w-b_{12}\frac{\partial\psi}{\partial x}-b_{13}\frac{\partial^2\Phi}{\partial x^2}=p+b_{14}\frac{\partial^2 V}{\partial x^2} \quad (17)$$

$$b_{31}\frac{\partial^2 w}{\partial x^2}+b_{32}\frac{\partial\psi}{\partial x}+\left(b_{33}\frac{\partial^2}{\partial x^2}+b_{35}\right)\Phi=b_{34}\frac{\partial^2 V}{\partial x^2} \quad (18)$$

where

$b_{11}=-b_{12}=2c_{55}hk$, $b_{14}=he_{15}$, $b_{42}=2\rho h$,

$b_{41}=-\dfrac{2h^3}{3}$, $b_{13}=\dfrac{4h}{3}e_{15}$, $b_{21}=-\dfrac{2h^3}{3}\left(\bar{c}_{11}-\dfrac{\bar{c}_{13}^2}{\bar{c}_{33}}\right)$,

$b_{22}=\dfrac{4h}{3}\left(\dfrac{\bar{c}_{13}}{\bar{c}_{33}}\bar{e}_{33}-\bar{e}_{31}\right)$, $b_{23}=-h\left(\dfrac{\bar{c}_{13}}{\bar{c}_{33}}\bar{e}_{33}-\bar{e}_{31}\right)$,

$b_{32}=-h\left[ke_{15}+\left(\bar{e}_{31}-\dfrac{\bar{c}_{13}}{\bar{c}_{33}}\bar{e}_{33}\right)\right]$, $b_{35}=\left(\dfrac{\bar{e}_{33}^2}{\bar{c}_{33}}+\bar{\varepsilon}_{33}\right)\dfrac{8}{h}$,

$$b_{31}=hke_{15},\quad b_{33}=-2h\varepsilon_{11}/3,\quad b_{34}=h\varepsilon_{11}/2 \quad (19)$$

The governing Eqs.(12), (13) and (14) are then transformed into Eqs.(16), (17) and (18). Noticing that k is the layerwise defined shear correction factor, which is introduced into the integration of τ_{xz} and D_x defined in Eq.(11).

SERIES SOLUTIONS FOR SIMPLY SUPPORTED BENDING

Generally, we consider a piezoelectric bimorph subjected to a uniformly distributed load or an electric potential applied to the top and bottom faces (Fig.2), and there is no surface density of moment m. The simply supported conditions for a rectangular beam with length l can be expressed as

$$w\big|_{x=0,l}=0\,,\ \sigma_x\big|_{x=0,l}=0\,,\ \phi\big|_{x=0,l}=0 \tag{20}$$

The electromechanical load functions of uniform distribution cases are written by Fourier series as

$$p(x,t)=\sum_{n=1}^{\infty}\left\{\frac{2p}{n\pi}\left[1-(-1)^n\right]\right\}\sin\left(\frac{n\pi}{l}x\right)\mathrm{e}^{\mathrm{i}\omega t} \triangleq \sum_{n=1}^{\infty}P_n\sin\left(\frac{n\pi}{l}x\right)\mathrm{e}^{\mathrm{i}\omega t} \tag{21a}$$

$$V(x,t)=\sum_{n=1}^{\infty}\left\{\frac{2V}{n\pi}\left[1-(-1)^n\right]\right\}\sin\left(\frac{n\pi}{l}x\right)\mathrm{e}^{\mathrm{i}\omega t} \triangleq \sum_{n=1}^{\infty}V_n\sin\left(\frac{n\pi}{l}x\right)\mathrm{e}^{\mathrm{i}\omega t} \tag{21b}$$

Then expanding the unknown functions in Eqs.(16), (17) and (18) with Fourier series yields

$$w(x,t)=\sum_{n=1}^{\infty}W_n\sin\left(\frac{n\pi}{l}x\right)\mathrm{e}^{\mathrm{i}\omega t} \tag{22a}$$

$$\psi(x,t)=\sum_{n=1}^{\infty}\Psi_n\cos\left(\frac{n\pi}{l}x\right)\mathrm{e}^{\mathrm{i}\omega t} \tag{22b}$$

$$\Phi(x,t)=\sum_{n=1}^{\infty}\Phi_n\sin\left(\frac{n\pi}{l}x\right)\mathrm{e}^{\mathrm{i}\omega t} \tag{22c}$$

Substituting Eqs.(21) and (22) into Eqs.(16), (17) and (18), yields the matrix form equations:

$$\begin{bmatrix} a_{11} & a_{12} & a_{13}\\ a_{21} & a_{22} & a_{23}\\ a_{31} & a_{32} & a_{33}\end{bmatrix}\begin{Bmatrix} W_n\\ \Psi_n\\ \Phi_n\end{Bmatrix}=\begin{Bmatrix} a_{14}V_n\\ P_n+a_{24}V_n\\ a_{34}V_n\end{Bmatrix} \tag{23}$$

where

$$a_{11}=-b_{11}\frac{n\pi}{l},\ a_{14}=(b_{14}-b_{23})\frac{n\pi}{l},\ a_{22}=b_{12}\frac{n\pi}{l},$$
$$a_{12}=-b_{21}\left(\frac{n\pi}{l}\right)^2-b_{12}+b_{41}\omega_n^2,\ a_{13}=(b_{22}-b_{13})\frac{n\pi}{l},$$
$$a_{24}=-b_{14}\left(\frac{n\pi}{l}\right)^2,\ a_{23}=b_{13}\left(\frac{n\pi}{l}\right)^2,\ a_{31}=-b_{31}\left(\frac{n\pi}{l}\right)^2,$$
$$a_{21}=b_{11}\left(\frac{n\pi}{l}\right)^2-b_{42}\omega_n^2,\ a_{32}=-b_{32}\frac{n\pi}{l},$$
$$a_{33}=-b_{33}\left(\frac{n\pi}{l}\right)^2+b_{35},\ a_{34}=-b_{34}\left(\frac{n\pi}{l}\right)^2 \tag{24}$$

Solving Eq.(23) for W_n, Ψ_n and Φ_n yields the Fourier coefficients in Eq.(22), based on which other related electromechanical variables are readily obtained. Furthermore, if the series arrangement is treated the same way as the parallel arrangement, one will find that the governing equations and solution expressions are exactly the same.

For free vibration, the right-hand side of Eq.(23) is set to zero, and nontrivial solutions for W_n, Ψ_n and Φ_n imply that the determinant of the coefficients matrix of Eq.(23) vanishes. Then solving Eq.(23) gives the resonant frequencies for a given n.

NUMERICAL RESULTS AND ANALYSIS

In this section, we will consider the free vibration of the bimorph with l=1 m and different thickness $2h$=0.01 m, 0.02 m, 0.05 m, 0.1 m, 0.2 m. The material properties of the layers for the numerical simulations are given in Table 1. To demonstrate the performance of present analytical FSDT model, the shear correction factor should be determined first. For explicitness, we adopt two commonly used values k=8/9 (Timoshenko, 1922) and k=5/6 (Cowper, 1966) for bimorphs in plane stress problems.

The frequencies of the resonant modes predicted by the present model with k=8/9 and k=5/6 for PZT-5A are plotted in Fig.3 for comparison with the

Table 1 Material constants of piezoelectric bimorph

Property	PZT-5A	Property	PZT-5A
c_{11} (GPa)	105	e_{31} (C/m^2)	−9.78
c_{12} (GPa)	54.6	e_{33} (C/m^2)	13.8
c_{33} (GPa)	86.8	e_{15} (C/m^2)	12.2
c_{13} (GPa)	52.7	ε_{11} (nF/m)	16.4
c_{55} (GPa)	22.2	ε_{33} (nF/m)	15.1
ρ (kg/m^3)	7800		

results provided by exact 2D theory. It is clear that rather good agreement is observed for the present model, and even for higher modes such as n=10. The error is smaller than 1% and 2% for the cases using k=8/9 and k=5/6, respectively. As expected, the errors of FSDT frequency estimation increase with the increasing of the mode order and aspect ratio of the bimorph.

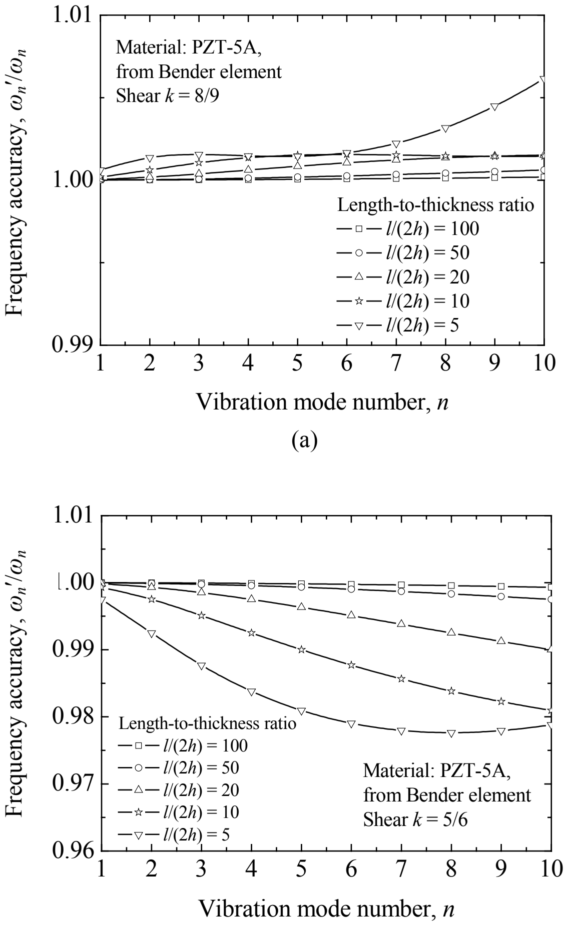

Fig.3 Frequency accuracy performance
(a) k=8/9; (b) k=5/6

Meanwhile, for the same n, the prediction accuracy for k=5/6 is lower than that for k=8/9 with increasing aspect ratio. The difference implies that the dynamic prediction based on FSDT is sensitive to the exactness of shear k. This phenomenon might be attributed to the shear stiffness (kGA) change from k variation, while the former is directly related to resonant frequencies.

CONCLUSION

In the present study, piezoelectric bimorph structures were investigated using FSDT approach mainly based on the principle of linear piezoelectricity and on the quasielectrostatic hypothesis. The model combines an equivalent single-layer approach for the mechanical displacements with a layerwise-type model for electric potential. The modelling process and numerical analyses revealed that:

1. Piezoelectric bimorphs will behave fundamentally the same way for both series and parallel arrangements under the same loading;
2. In dynamic analysis, high accuracy of bending vibration frequencies can be obtained by the present model even for rather thick beam (Aspect ratio=5), whereas classical elastic thin beam or plate theory gives less accurate results;
3. In FSDT model, shear correction factor plays a key role in ensuring the prediction accuracy of dynamic response, and choosing the appropriate k value for piezoelectric laminates is worth further investigation when using FSDT approaches.

ACKNOWLEDGEMENT

The authors would like to express their gratitude to Dr. Hui-ming Wang and Prof. Wei-qiu Chen, of Zhejiang University, for their helpful advice and comments on this paper.

References

Chee, C.Y.K., Tong, L., Steven, G.P., 1998. A review on the modeling of piezoelectric sensors and actuators incorporated in intelligent structures. *Journal of Intelligent Material Systems and Structures*, **9**:3-19.

Cowper, G.R., 1966. The shear coefficient in Timoshenko's beam theory. *Journal of Applied Mechanics*, **33**:335-340.

Ding, H.J., Wang, G.Q., Chen, W.Q., 1997. Green's functions for a two-phase infinite piezoelectric plane. *Proceedings of the Royal Society Series A*, **453**:2241-2257.
Fernandes, A., Pouget, J., 2003. Analytical and numerical approaches to piezoelectric bimorph. *International Journal of Solids and Structures*, **40**:4331-4352.
Gopinathan, S.V., Varadan, V.V., Varadan, V.K., 2000. A review and critique of theories for piezoeletric laminates. *Smart Materials and Structures*, **9**:24-48.
Ha, S.K., Kim, Y.H., 2002. Analysis of a piezoelectric multi-morph in extensional and flexural motions. *Journal of Sound and Vibration*, **253**(5):1001-1014.
He, L.H., Lim, C.W., Soh, A.K., 2000. Three-dimensional analysis of an antiparallel piezoelectric bimorph. *Acta Mechanica*, **145**:189-204.
Lim, C.W., He, L.H., Soh, A.K., 2001. Three-dimensional electromechanical responses of a parallel piezoelectric bimorph. *International Journal of Solids and Structures*, **38**:2833-2849.
Rao, S.S., Sunar, M., 1994. Piezoelectricity and its use in disturbance sensing and control of flexible structures: a survey. *Applied Mechanics Reviews*, **47**:113-123.
Shirley, D.J., Hampton, L.D., 1978. Shear-wave measurements in laboratory sediments. *Journal of the Acoustic Society of America*, **63**(2):607-613.
Smits, J.G., Dalke, S.I., Cooney, T.K., 1991. The constituent equations of piezoelectric bimorphs. *Sensors and Actuators A-Physics*, **28**:41-61.
Sosa, H.A., Castro, M.A., 1993. Electroelastic analysis of piezoelectric laminated structures. *Applied Mechanics Reviews*, **46**:21-28.
Timoshenko, S.P., 1922. On the transverse vibrations of bars of uniform cross-section. *Philosophical Magazine*, **6**(43): 125-131.
Timoshenko, S.P., Yong, D.H., Weaver, W., 1974. Vibration Problems in Engineering (4th Ed). Wiley, New York.
Wang, Q., Quek, S.T., Sun, C.T., Liu, X., 2001. Analysis of piezoelectric coupled circular plate. *Smart Materials and Structures*, **10**:229-239.
Wang, S.Y., 2004. A finite element model for the static and dynamic analysis of a piezoelectric bimorph. *International Journal of Solids and Structures*, **41**:4075-4096.
Yang, J.S., 1999. Equation for thick elastic plates with partially electroded piezoelectric actuators and higher order electric fields. *Smart Materials and Structures*, **8**:73-82.
Zhou, Y.G., Chen, Y.M., Huang, B., 2005. Experimental study of seismic cyclic loading effects on small strain shear modulus of saturated sands. *Journal of Zhejiang University SCIENCE*, **6A**(3):229-236.

APPENDIX A

The 3D constitutive equations applied to an orthotropic piezoelectric material can be written in its material axes (1, 2, 3), using the usual condensed (engineering) notations for the material constants as

$$\sigma_{ij} = C_{ij}S_j - (-1)^r e_{ji}E_j\,,\ D_i = (-1)^r e_{ij}s_j + \varepsilon_{ij}E_j \quad \text{(A1)}$$

where r is an integer mentioned in the main text; σ_{ij} and S_j are the components of the stress tensor and the strain; E_i and D_i the components of the electric field and electric displacement components; C_{ij}, e_{ji} and ε_{ij} the elastic stiffness components, the piezoelectric coefficients and the dielectric constants, and they are

$$[C] = \begin{bmatrix} c_{11} & c_{12} & c_{13} & 0 & 0 & 0 \\ c_{12} & c_{22} & c_{23} & 0 & 0 & 0 \\ c_{13} & c_{23} & c_{33} & 0 & 0 & 0 \\ 0 & 0 & 0 & c_{44} & 0 & 0 \\ 0 & 0 & 0 & 0 & c_{55} & 0 \\ 0 & 0 & 0 & 0 & 0 & c_{66} \end{bmatrix},$$

$$[e] = \begin{bmatrix} 0 & 0 & e_{31} \\ 0 & 0 & e_{32} \\ 0 & 0 & e_{33} \\ 0 & e_{24} & 0 \\ e_{15} & 0 & 0 \\ 0 & 0 & 0 \end{bmatrix},\quad [\varepsilon] = \begin{bmatrix} \varepsilon_{11} & 0 & 0 \\ 0 & \varepsilon_{22} & 0 \\ 0 & 0 & \varepsilon_{33} \end{bmatrix} \quad \text{(A2)}$$

For 2D plane problems, introducing the plane stress assumptions (i.e., σ_{22}=0, σ_{23}=0, σ_{12}=0, D_2=0) into Eq.(A1), and solving σ_{22}=0 for s_{22} gives

$$s_{22} = -\frac{1}{c_{22}}\left[c_{12}s_{11} + c_{23}s_{33} - (-1)^r e_{32}E_{33}\right] \quad \text{(A3)}$$

Substituting Eq.(A3) into Eq.(A1) yields Eq.(2). And the reduced material constants under plane stress assumptions are given by

$$\bar{c}_{11} = c_{11} - c_{12}^2/c_{22}\,,\ \bar{c}_{13} = c_{13} - c_{12}c_{23}/c_{22}\,,$$
$$\bar{c}_{33} = c_{33} - c_{23}^2/c_{22}\,,\ \bar{e}_{31} = e_{31} - c_{12}e_{32}/c_{22}\,,$$
$$\bar{e}_{33} = e_{33} - c_{23}e_{32}/c_{22}\,,\ \bar{\varepsilon}_{33} = \varepsilon_{33} + e_{32}^2/c_{22} \quad \text{(A4)}$$